UDK621.3:(53+54+621+66), ISSN0352-9045

DIRECT BONDING OF (111) AND (100) ORIENTED SILICON WAFERS

Drago Resnik, Danilo Vrtačnik, Uroš Aljančič and Slavko Amon
Laboratorij za Mikrosenzorske strukture, Fakulteta za Elektrotehniko, Ljubljana, Slovenia

Keywords: semiconductors, silicon wafers, bonding, direct bonding, surface roughness, crystal orientation dependent bonding, bond tensile strength, voids, MEMS, MicroElectroMechanical Systems, MM, MicroMachining

Abstract: Wafer bonding of commercially available (100) and (111) silicon wafers was performed in the range of temperatures from 80°C to 400°C in nitrogen, oxygen and low vacuum atmosphere. Surface preparation with modified RCA cleaning method and hot nitric acid provided extremely clean and hydrophilic surfaces that were later brought into intimate contact. Bonding quality evaluated by the tensile strength measurements showed the highest values reaching 18 MPa. Correlation between prebonding treatment, initial surface roughness and microroughness was made revealing the influence on the bonding energy. (111) oriented wafers exhibited higher bonding abilities compared to (100) in case of bonding wafers with native oxides. This is believed to be due to higher density of available bonding sites as a consequence of enhanced chemical oxide growth rate and its homogeneity on (111) surface. Moreover, it is believed that due to higher positive charge of oxides grown on (111) oriented silicon compared to (100), desorption of interfacial water is accelerated, thus increasing the bonding energy at lower temperature. Interface imperfections of bonded samples were investigated by infrared transmission imaging revealing bubbles at the bonded interface only in case when bonding was performed in oxygen ambient.

Various combinations of surface terminations such as thin chemical native silicon dioxide and thick thermal silicon dioxide on (111) and (100) oriented silicon wafers were prepared and investigated. In conclusion, the best bonding results were obtained by bonding (100) wafers with thick thermal oxide to (111) wafers with native oxide and annealed in nitrogen ambient. Bonding of silicon pressure sensor on (111) oriented substrate was finally performed as a practical example of application of this bonding technique.

Direktno bondiranje silicijevih ploščic orientacije (100) in (111)

Ključne besede: polprevodniki, rezine silicijeve, bondiranje, bondiranje neposredno, hrapavost površin, bondiranje odvisno od orientacije kristalov, trdnost natezna bondov, praznine, MEMS sistemi mikroelektromehanski, MM obdelava najfinejša

Povzetek: Medsebojno spajanje ali takoimenovano "bondiranje" silicijevih ploščic kristalnih orientacij (100) in (111) je bilo izvedeno pri temperaturah med 80 in 400°C v treh različnih atmosferah: dušiku, kisiku in pri nizkem vakumu (10 Pa). Priprava silicijeve površine je bila izvedena z modificirano metodo klasičnega RCA čiščenja, ki se uporablja v mikroelektroniki ter naknadno pripravo površine v dušični kislini pri 70 in 110°C. Tako smo dobili izjemno čisto površino brez delcev in ostalih nečistoč, obenem pa kemijsko zaključeno s tanko plastjo silicijevega oksida, torej hidrofilno površino. Po fizičnem spajanju silicijevih vzorcev pri sobni atmosferi in temperaturni obdelavi so bili narejeni testi natezne trdnosti spojenih vzorcev. Trgalni preizkusi so pokazali dosežene vrednosti do 18 MPa. V članku so nadalje podane korelacije med začetno hrapavostjo silicijevih vzorcev ter vplivom čiščenja na slednjo in natezno trdnostjo spojev. Silicijevi vzorci (111) orientacije so pokazali večje natezne trdnosti v primerjavi z (100) vzorci za primer, če so bile spajane površine zaključene s kemijskim oksidom. To je verjetno zaradi večje gostote vezi na (111) silicijevi površini, kar ima za posledico bolj homogeno in hitrejšo rast kemijskega oksida na površini. Nadalje se lahko sklepa, da je desorpcija molekul vode iz spojne površine povečana tudi zaradi večjega pozitivnega naboja v oksidu, ki zraste na površini (111). To naj bi bil dodaten vzrok za povečanje bondirne energije pri nizkih temperaturah. Poleg zaključitve površine s tankim kemijskim oksidom je bila pripravljena tudi površina z debelejšim termično raščenim oksidom (253nm). Pokazano je, da je bondiranje najbolj uspešno ravno v primeru, če ima ena površina tanek kemijski oksid, druga pa debelejši termični oksid. Na podlagi teh ugotovitev je bilo izvedeno bondiranje silicijevega senzorja tlaka na silicijevo podlago (111) orientacije.

1. Introduction

Wafer bonding refers to a mechanical fixation of two or more wafers to each other by intermolecular forces between them. Direct fusion bonding of silicon wafer pairs was in detail first reported by Lasky more than a decade ago for the purpose of SOI technology /1/ and by Shimbo on the formation of bonded pn diode /2/. However, with progressive development of silicon micromachining, bonding at waferscale has also become a very essential technique in advanced silicon micromachining and fabrication of microsystems. Sensors and actuators as well as other microelectromechanical systems (MEMS) realized by micromachining are mounted usually on a rigid substrate, whether due to assembly purpose or due to their functionality requirements. Some of them require hermetically sealed cavities, for example absolute pressure sensors while others utilize bonding to realize multilayered structures such as micropumps, microvalves or similar.

Bonding in generally is however not restricted only to silicon but in this work only this subject will be considered. For instance silicon wafers can be bonded by electrostatic bonding to glass with matched thermal expansion coefficients such as Pyrex 7740 /3/. Low temperature bonding with intermediate layers of binding PSG glass, frit glasses, metals or polymers is also used in many cases, but has inferior performances regarding stability and hermetical sealing /4/. To exclude thermal mismatch, bonding of silicon wafer to another silicon wafer is an appropriate solution. We distinguish between silicon to silicon direct fusion bonding which takes place at high temperatures (900°C-1000°C) and direct bonding at low temperatures (below 400°C). The first approach requires high temperature

step that many devices built on the wafer can not withstand, while the second one exhibits some inferior bonding performances such as lower bonding energy and presence of voids at the bonding interface. Progress made in recent years with emphasis on surface preparation techniques brought the bonding energies close to those achieved with high temperature processes.

Among several techniques used in bonding active silicon wafer (wafer with prefabricated circuitry or microstructures) on silicon support wafer, low temperature bonding /5-15/ is emerging as a very promising one due to the following facts:

- no intermediate layers are needed (no thermal expansion mismatches)
- no external electrical field is applied (possible active circuitry damage is avoided)
- no high temperature steps (enabling bonding of finished metalized structures)

Many low-temperature direct bonding approaches and techniques were recently proposed with different bond quality and application suitability. They are dealing with bonding in ultraclean environment /17/, bonding in low vacuum range /14/, ultra high vacuum at room temperatures /10,11,16/, etc. While many are based on wet chemical surface preparation, some propose appropriate in-situ preparation of hydrophilic surface with oxygen plasma /11/ or argon high energy beam surface etching /10/. From the practical and environmental point of view it is expected that dry cleaning methods in vacuum will probably prevail over wet chemical methods or a combination will persist. Despite all, one must not forget that bonding has to be a robust, reproducible and cost effective production oriented process. Excellent results were recently reported by Satoh, who performed bonding with aid of thin film of water glass at 80°C /34/. In this place a very extensive survey report by Plössl should be mentioned, containing numerous references from this field /35/.

This paper addresses some relevant issues in silicon wafer bonding such as surface roughness, wafer orientation, surface preparation and the impact these parameters have on bond quality.

In silicon micromachining, support bonding wafer is commonly of (111) or (100) crystal orientation, P or N type, but does not exclude also some other materials and crystal orientations. It has to comply with the process and assure appropriate bonding quality for the specific application. Our research was focused mainly on bonding differently prepared hydrophilic surfaces of (111) and (100) oriented silicon wafers using low temperature processes (80°C-400°C) under three distinct ambient conditions: N2, O2, and low vacuum in order to compare their bonding performances. The aim of this work was to achieve a high bonding energy by covalent bridging between two mating hydrophilic silicon surfaces at low temperature using the chemicals which do not attack any layer of the finished device.

2. Bonding mechanism

During the last ten years, many models were proposed by different authors /1,23,24,25/. The model recently proposed by Tong and Gösele /25/ offers a very concise and consistent insight into bonding mechanism and it is primarily based on the fact that surfaces brought together are originally prepared hydrophilic, i.e. covered with silanol groups which act as adsorption sites for water molecules. It is now widely accepted that silicon surface hydrophilicity, caused by hydroxyl groups and physisorbed water, plays a major role in the process of bonding two silicon surfaces. Hydrophilic nature of the silicon surface can be obtained either by oxygen plasma activation or by wet oxidizing agents (sulfuric acid, nitric acid, SC1 cleaning solution,..). The schematic presentation of termination of two hydrophilic surfaces in contact as shown by Weldon is presented in Fig.1.

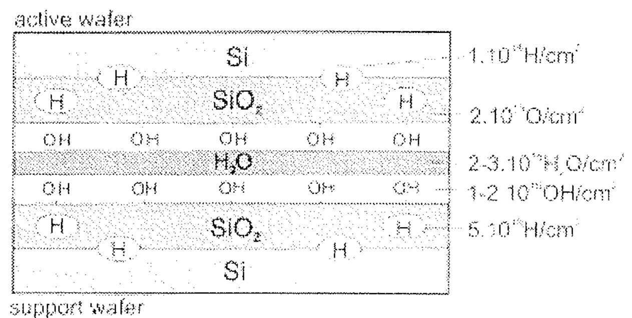

Fig.1: Depiction of bonding interface region of two hydrophilic silicon surfaces as presented by Weldon /29/.

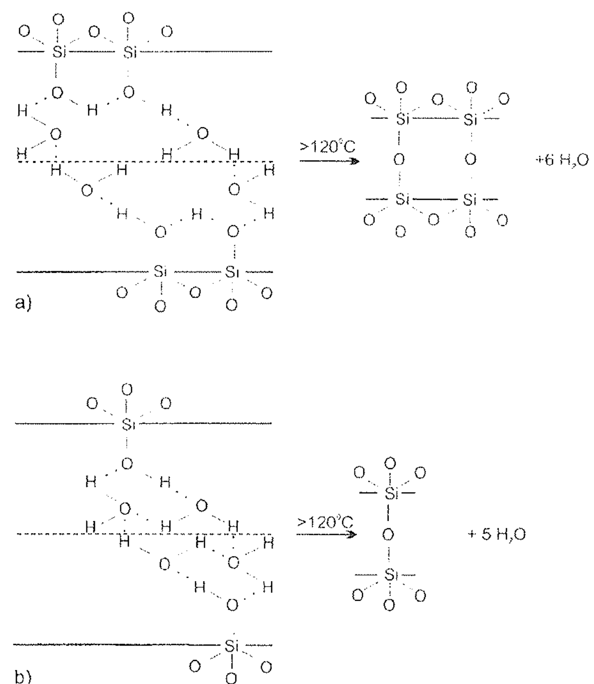

Fig. 2: Bonding model by Tong /25/, showing bridging of two hydrophilic silicon surfaces at room temperature and subsequent transform to siloxane bonds at elevated temperature with excess water. Both types of OH groups, a) isolated and b) associated are acting simultaneously.

Model of Tong and Gösele is presented in Fig. 2 and illuminates the bonding by the following explanation. At room temperature and relative humidity of 45%, hydrophilic surface is inevitably additionally covered with few monolayers of water molecules attached to OH groups via hydrogen bonds. After bringing two hydrophilic surfaces into intimate contact it was also observed that the wafers can be separated by blade and moreover the bond can be restored again. For example, it was shown by Bäcklund that hydrophobic surfaces (only Si-H terminated surface) also stick together /28/, while Weldon further showed by infrared absorption spectroscopy that only hydrogen terminated surfaces stick together via Van der Waals forces /29/. This could not be confirmed for hydrophilic surfaces /29/. Room temperature bonding of two hydrophilic surfaces in our case is presumably taking place by hydrogen bonds between opposite water molecules groups. Tong model in Fig. 2 shows water bridging between two surfaces via isolated and hydrogen-bonded associated OH groups. By taking into account saturated density of both silanol groups, surface energy of $165 mJ/m^2$ was calculated, that is in agreement with measured results.

Energetically favorable rearrangement of bonds occurs at subsequent bond annealing or strengthening above 130°C. The temperature range 130°-150°C is consistent with the fact that most of the water is removed from the interface at this temperature and appreciable polymerization of silanol groups across the interface occurs via hydrogen bridges (Eq.1). Si-O-Si covalent bonds are starting to form with interfacial water as a byproduct. On the other hand water molecules cause partial slow fracture of Si-O-Si bonds, which are chemically more active by the presence of stress in strained hydrous oxide layer as shown by Michalske-Freiman model /31/. Consequently this reaction in reverse direction causes increased number of Si-OH groups (Eq. 1). Desorption of water at this temperature is however not complete and some water (20%) is still present at bonding interface up to 400°C /29/. Based on the previous facts we believe that water acts via two mechanisms in the reaction as follows from Eq.1 and reenters the process via Eq. 2 (dissociation and oxidation as confirmed by IR spectroscopy by Weldon /29/). It is our believe that bonding is also orientation dependent, taking into account different growth rate mechanism of chemical oxide on two orientations under investigation.

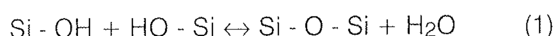

$$Si-OH + HO-Si \leftrightarrow Si-O-Si + H_2O \qquad (1)$$

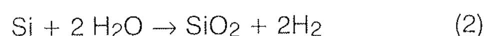

$$Si + 2H_2O \rightarrow SiO_2 + 2H_2 \qquad (2)$$

If interface water is successfully removed from interface via outdifusion, what is less probable, or time and temperature dependent dissociation takes place, then strong siloxane bonds are formed. Interfacial species must either react at the interface or dissolve into the oxide and bulk in order to allow the oxides to mate tightly. If water is trapped at the interface, bubbles are formed as described by several authors /6,17,24,32/. For unbonded part of the area a term bubble or void is normally used. Water within bubbles can play a role at elevated temperatures via enhanced dissociation process thus releasing pressure which makes the bubbles to finally disappear. However they simultaneously generate from other reasons, possible sources being hydrogen from dissociation process (Eq. 2) or vaporized hydrocarbons (CH_x). This was studied in detail by Mitani, showing that all three origins can take place simultaneously in bubble formation process /17,32/. Solutions to this problem were proposed such as wafer preheating to desorb hydrogen or cleaning to remove hydrocarbons, while for water removal, bonding in high vacuum was suggested /10/.

Wet oxidizing treatment of clean hydrophobic silicon surface in hot HNO_3 proceeds via chemical reaction according to Eq. 3 rendering not only the growth of strained native oxide with sufficient density of attached silanol groups, but also removes hydrocarbons from the surface /5/. Due to gaseous NO reaction product, trapped in porous chemical oxide long rinsing in DI water is mandatory to remove all traces.

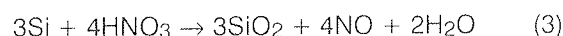

$$3Si + 4HNO_3 \rightarrow 3SiO_2 + 4NO + 2H_2O \qquad (3)$$

Hattori showed that the structure of this oxide can be characterized by the distribution of Si^{3+} suboxide and that the correlation to Si-H bond density can be established. This correlation explains that enhanced formation rate of native oxide in nitric acid is due to increased mobility of oxidizing species through present Si-H network which terminates the surface prior to hydrophilisation. Distribution of Si^{3+} is uniform in contrast to other hydropylisation chemicals which result in a piled up distribution at the interface /19/. This was also confirmed by Jiao, who reported that beside sufficient Si-OH also Si-H surface terminations are found simultaneously on the surface /8/. Aoyama et al. have showed by selective etching with photoexcited fluoride and by STM observations that SiO_2 formed in HNO_3 or SC1 is not a uniformly thick layer, but has rather an island structure, with some islands connected mutually together, thereby confirming the existence of both Si-OH and Si-H surface termination appearing simultaneously. Pinhole density of such chemically prepared oxides was estimated to $5x10^9$ per cm^2 /27/. With oxygen plasma treatment, the desorption of undesired adsorptives and the activation of free sites for the adsorption of OH groups is achieved simultaneously. Treatment in plasma results in highly reactive and thus fully hydrated surface and exhibits long term stability of hydrophilic surface nature /9,26/.

From our observation it was determined that the growth of native oxide in nitric acid at 70°C renders the bonding strength lower compared to the oxides grown at 110°C. We suggest that this is due to nonhomogeneous oxide layer growth with more pinholes and consequently less OH bonding sites at the interface.

In case of (111) wafers, the growth of chemical oxide is enhanced or at least more homogeneous compared to (100) orientated wafers due to lower steric hindrance of surface atoms. This imposes superior bond results in case of (111) oriented wafers as will be shown in the results later. We believe that there also exists influence of positive oxide charge, which influences the water molecule dipole attraction force /24/. As it is known from MOS theory, oxides grown on (111) substrate exhibit about one order higher positive fixed charge than oxides grown on (100) substrates. Stronger hydrophilic

nature of bonding surface, due to higher positive charge in oxides grown on (111) surface as compared to (100), could be an additional reason for subsequently strengthening the bond via temperature dependent process of water desorption from interface.

3. Experimental

Standard, commercially available Czochralsky grown, one side mechanically polished 3" silicon wafers of (100) and (111) orientation were used in our studies. Resistivity of wafers was 10-20 Ωcm, while thickness was 380μm. In order to bond wafers successfully special attention has to devoted to the following three fundamental steps:

- surface preparation to obtain clean, particle free, smooth and hydrophilic surface
- prebonding at room temperature in air to join and accommodate two surfaces with specific surface roughness
- bond annealing (strengthening) at elevated temperature in appropriate ambient to obtain covalent siloxane bonds between two wafers

3.1 Surface preparation

Cleaning of the silicon surface has a great impact on surface chemistry and topography /18/. To mitigate the surface roughening occurring during RCA standard cleaning (SC1) treatment, diluted SC1 was used as described in Table 1. In this stage, a trade off between cleaning efficiency and surface roughening has to be achieved. Surface roughening was monitored by AFM measurements. As it can be seen from Table 1 modified RCA cleaning was followed by oxide removal in diluted HF to expose silicon surface and rinse in deionized (DI) water. At this point dry wafers were immersed into hot nitric acid (HNO_3) at 70°C or 110°C, allowing growth of few monolayers of fresh hydrous chemical oxide. After prolonged DI water rinsing wafers were dried with hot nitrogen and the surface preparation was hence completed. Following the procedures described in Table1 we obtained a hydrophilic, OH terminated silicon surface /8/. Since the surface during cleaning is very prone to the attraction of particles, special care must be taken when performing these steps. Particle free silicon surface is essential in performing successful bonding task, therefore all the work was performed in cleanroom ambient of class 10. In Table 2 data concerning the wafer pairing combinations by orientation, surface preparation of paired wafers and thickness of layers on the prebonding surfaces are presented. Thickness of oxide layers was measured on parallel test wafers as a difference between ellipsometric measurement prior to and after nitric acid treatment. The values were in agreement with data of other authors /19/. Samples with thermal oxide were prepared by wet thermal oxidation atmosphere at 975°C.

3.2 Prebonding at room ambient

Prebonding step has to follow immediately after surface preparation. Two wafers were put into intimate contact by use of teflon fixture in cleanroom ambient and room temperature. It was also found important to initiate bonding in the center by locally pressing the center region from the top, thus enabling bonding phenomenon to propagate radially thus confirming the work of Tong /5/. The aim of this operation is to squeeze out the air cushion between surfaces, thereby preventing any air trapping at the bond interface. Following this operation, pressure in the range of 0.1MPa was applied homogeneously across the entire wafer area for dura-

Table 1. Surface preparation of silicon wafers

RCA cleaning - modified @ 70°C, 10 min, SC1- (0.25 NH_4OH :1 H_2O_2 : 5 H_2O) DI, 10 min HF* : H_2O 1 : 100 @ 25°C, 5 min DI, 10 min HNO_3* @ 70 or 110°C, 15 min DI, 30 min
*HF 50% VLSI Puranal Riedel de Haen *HNO_3 70% VLSI Puranal Riedel de Haen

Table 2. Experimental data of silicon wafer pairing combinations and surface termination prior to bonding

No.	Bond wafer pairing combinations	Temperature of HNO_3 in native oxide growth [°C]	Surface layer thickness before prebonding [nm]
1	(100) / (111)	110°C / 110°C	0.8-1 / 0.9-1.2
2	(100) / (100)	110°C / 110°C	0.8-1 / 0.8-1
3	(111) / (111)	110°C / 110°C	0.9-1.2 / 0.9-1.2
4	(100) / thermal oxide	110°C / none	0.8-1/ 253
5	(111) / thermal oxide	110°C / none	0.9-1.2 / 253
6	(100) / (111)	70°C / 70°C	0.5 / 0.6

tion of 10 seconds. According to the findings of Tong et al., these mated samples were afterward stored for a period of 150 hours in inert ambient at room temperature to reach the saturated value of interface energy /5/.

It is known that effective bond area and consequently overall bonding energy can be increased by applying external static pressure which increases the surface energy to a value defined by a number of available bonding sites /15/. By doing this we actually help to accommodate the two surfaces that suffer from nonflatness via elastic deformation process, as described by Maszara /30/. Higher pressure of 1.5 MPa was also applied to some samples, but no gain in bond quality was observed. After this prebonding procedure was completed, the bond was in all cases sufficiently strong to withstand the dicing of bonded wafers into smaller samples for providing further temperature dependent tests.

3.3 Bond annealing

The final step in low temperature bonding is bond annealing (also termed strengthening), when transformation of silanol to strong siloxane bonds takes place at elevated temperature above approximately 130°C as will be shown in results. Bond strengthening was performed at different temperatures in the range from 80°C to 400°C, and in different ambients. Thermal treatments were performed in Tempress junior furnace in the case of nitrogen and oxygen atmosphere while for low vacuum at 10 Pa bond strengthening in vacuum furnace was performed with two stage vacuum pump and oil backstreaming trap to prevent contamination. The duration of this step was 60 minutes in all cases. This parameter was chosen according to the results of Berthold who found minor influence of prolonged bond strengthening on bonding energy /7/. This was confirmed also by Stengl /23/. In this temperature range further accommodation of two surfaces occurs via elastic deformations at microroughness scale.

3.4 Bond characterization methods

Fig. 3 shows principally the measurements of tensile strength of bonded samples by pull test method /6/, while Fig.4 shows a setup for bond characterization by infrared transmission imaging for detecting voids and imperfections, which was applied also by others, but with modifications /20,21/. In our case IR camera model PTC-10A was used. These are two most commonly used criteria in the bond quality evaluation. Also X-ray

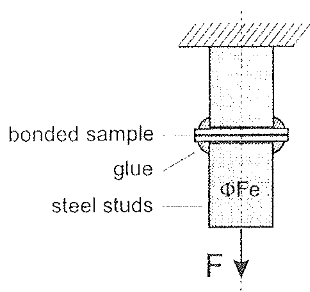

Fig. 3: Tensile strength measurement principle for evaluation of bonded silicon samples.

diffraction topography method, same as used for welding inspection was utilized for the purpose of void detection and resolution comparison. Another method used to reveal microvoids at the interface was cross-sectioning by dicing of bonded samples followed by short isotropic etch. For the purpose of tensile strength characterization 10x10 mm^2 samples were prepared to fit the requirements of pull test apparatus. The samples were glued on steel studs by cyanoacrylate UHU-plus 300. The studs with samples were attached in Amsler 20kN pull tester and the tensile force of breakage was determined. To avoid inconsistent results ten samples of each process variation were tested.

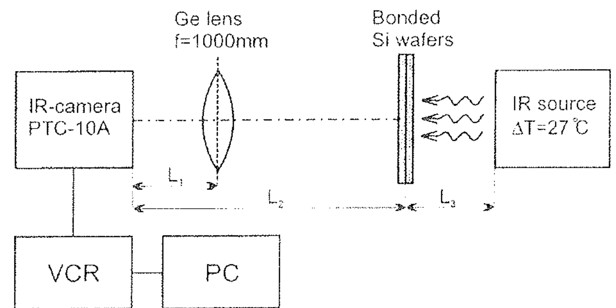

Fig. 4: Setup for bond characterization by IR transmission method applied in our work.

4. Results and discussion

Parameters that mainly influence bond quality of bonded hydrophilic silicon wafers are generally recognized as: i) surface cleanliness, ii) saturated surface hydrophilicity and iii) surface roughness and nonflatness. Surface cleanliness was controlled under UV inspection light and generally no particles were observed with naked eye. To evaluate the degree of hydrophilicity, water drop contact angle measuring method was used /26,28/. Immediately after surface preparation, shown in Table 1 measured angles were between 2° and 4°. Bond quality dependence on surface roughness origins, annealing ambient, wafer orientation and surface termination are discussed in the following subsections.

4.1. Surface roughness of bonded silicon

To find a possible correlation between the silicon surface microroughness and bond quality we performed several roughness and microroughness measurements with Taylor-Hobson Tallysurf Series 2 surface profiler and Park Scientific Instruments atomic force microscope (AFM), respectively. Attention was paid not only to the initial roughness, but also to the roughness contribution from the cleaning method as well as role of surface roughness in bonding process.

The theoretical model of Maszara, revealing the possible way of bonding two surfaces with nonideal flatness helped to gain better insight into the stresses present in the bonded wafers /30/. Matching of the two interfaces acts via elastic deformation of each wafer that are macroscopic in the case of nonflatness and micro-

scopic in case of microroughness. Most deformation occurs at room temperature prebonding step. Wafer thickness plays also important role in stress release distribution and deformation. Thinner wafers would allow bonding of more rough surfaces via deformation processes. Stresses due to bonding are a combination of tensile, compressive and shear stress and are decaying from the interface to the bulk of the wafers.

To allow intermolecular forces to be active, particularly hydrogen bonds in our case, mating surfaces have to be in a sufficient proximity, calculated to be below 1nm /25/. That´s why particularly wafer nonflatness at room temperature prebonding and microroughness at annealing temperatures, are important issue in wafer bonding. Closing the gap between the two bonding surfaces that is a consequence of nonflatness is possible if following criterion from the theory of deformations is fulfilled /17/.

$$\frac{h}{r^2} < \sqrt{\frac{\gamma}{Et^3}} \qquad \text{Eq.1}$$

where h is the height of asperities, r is the length of lateral distance between asperities, γ is the interface energy (J/m^2) E is the Young´s modulus ($1{,}66\ 10^{11}$ Pa for (100) silicon) and t is the thickness of the wafer. For values of h measured in our case (above 60nm) elastic deformations can accommodate two surfaces though even higher values have been reported /35/.

Roughness measurements on our samples have shown that in the worst case we are dealing with three distinct orders of roughness on the same wafer, differing in amplitude and in spatial periodicity.

- First order roughness (also termed nonflatness or waviness) after SC1 cleaning appeared with spatial periodicity of 50-70 μm and peak-to-peak values of 60nm. First order roughness as shown in Fig.5 and found only at vendor A was found to be the origin of unsuccessful bonding of wafers, independently of surface preparation or bond strengthening conditions. Most of samples were broken during mounting in pull test apparatus while some showed inferior tensile bond strength of 0.1-0.3 MPa. Waviness is a consequence of the wafer dicing misalignment with respect to (100) plane and poor polishing procedure.
- Measured second order roughness that appeared with all the wafers from vendor A and B had a spatial period of 3-4 μm and peak-to-peak values of 20-30 nm and is presented in Fig. 6. By comparing the results from Fig. 5. and Fig. 6. that are actually two different silicon wafer vendors being involved in our work, we found the same second order roughness, but the absence of first order roughness in case of vendor B. It was determined during experiments that both roughness components are insensitive to the cleaning procedure and are mainly a consequence of tribomechanical polishing. The spatial period is attributed to the size of Syton colloidal silica particles.

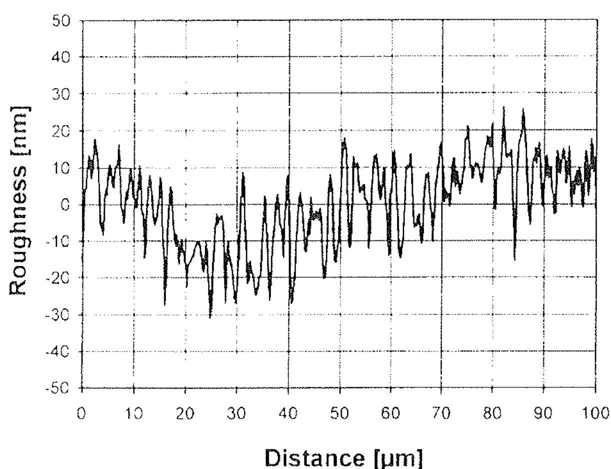

Fig. 5: Measured roughness profile of (100) wafer surface from vendor A. Second order waviness is normally observed but modulation with first order component with long period is significantly pronounced in this particular case.

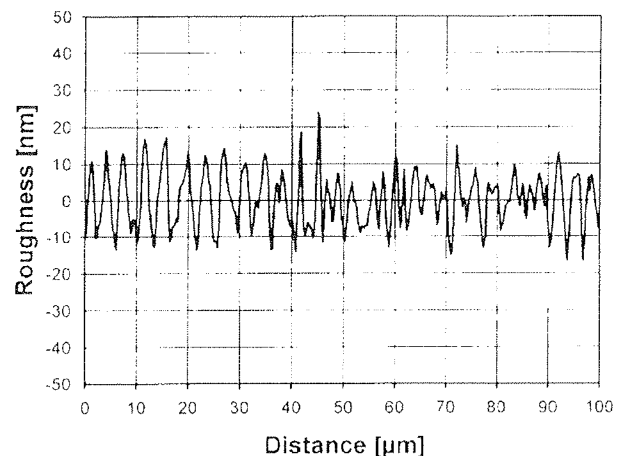

Fig. 6: Measured initial roughness profile of (100) surface from wafer supplier B, used in most of our experiments. Second order waviness is in the same range as in the previous diagram, but no first order roughness component is present.

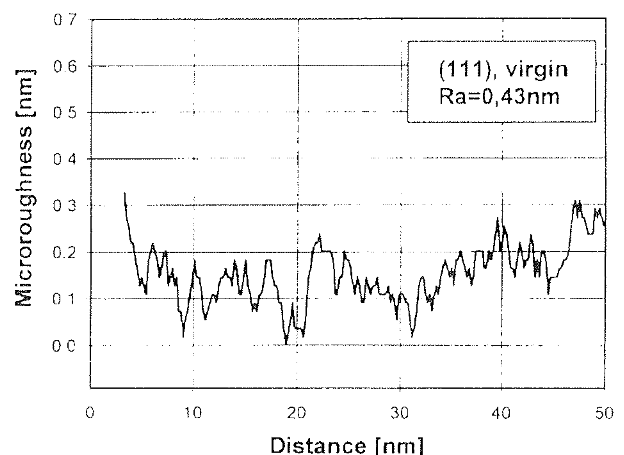

Fig. 7: AFM 2D microroughness profile of (111) "as delivered" virgin wafers from vendor B before SC1 cleaning.

- Third order roughness (termed also microroughness) was determined by AFM measurements and is on the atomic scale. Initial microroughness of "as delivered" wafers was in the range of Ra=0.38-0.43 nm for the case of (111) wafers from vendors A and B. 2D surface roughness profile is shown in Fig. 7. Almost similar was observed as well for (100) oriented wafers.

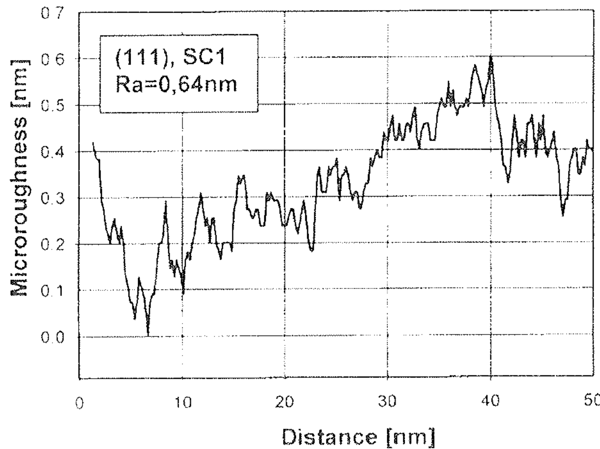

Fig. 8: AFM microroughness profile of (111) wafer surface from Fig. 7. after modified SC1 cleaning.

It was shown by Miyashita that according to different cleaning treatments, microroughness can increase by a factor of two or more /18/. By preserving the smoothness with diluting SC1 cleaning solution, we also decreased the particle removal efficiency. By analyzing the results of microroughness obtained by measurements with AFM and shown in Fig. 4-7 and the bond tensile strength results shown later, it was confirmed that the chosen cleaning was an appropriate trade off and roughening has not affected the bond quality. We investigated both, (100) and (111) surfaces and no significant difference in microroughness was observed between them. Microroughness of the same wafers as shown in Fig. 7 increased after modified SC1 cleaning and diluted HF dip to the values Ra=0.5-0.64 nm, corresponding to Fig. 8.

In Fig. 9 and Fig.10 are presented 3D AFM plots, showing the surface profile of (100) wafers before and after cleaning, respectively. The microroughening was slightly more pronounced for (111) surface, but this could be also due to difference in initial microroughness. Surface area of 0,05x0,05 μm^2 was analyzed showing minor differences in microroughness, ranging between Ra=0,089-0,16 nm.

By considering the generally accepted polishing standards in microelectronics, we found out that they completely satisfy the requirements of wafer bonding. First order roughness from Fig. 5 was more an exception to the rule. On the basis of our experimental results we suggest that for successful bonding, waviness (first order roughness) about 60nm and spatial period of 50-60 μm was already critical in our case. Intermolecular forces were probably not sufficiently strong to induce elastic deformations because of pronounced nonflatness for the wafer thickness involved.

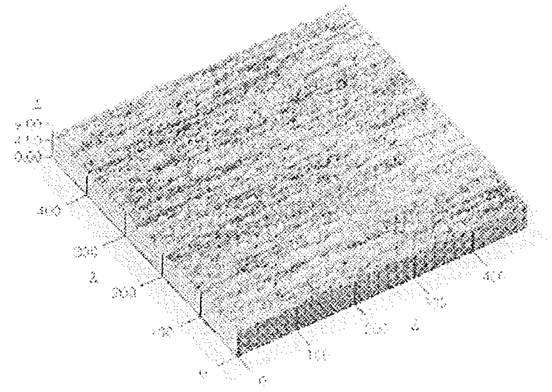

Fig. 9: Measured 3D microroughness profile of (100) wafer surface by AFM from vendor B before modified SC1 cleaning on 50x50nm^2 area.

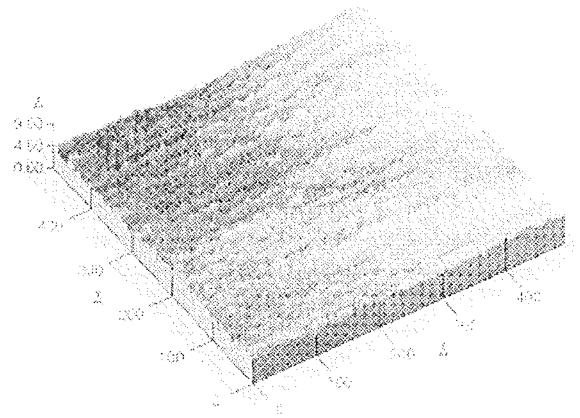

Fig.10: Measured 3D microroughness profile of (100) wafer surface by AFM from vendor B after modified SC1 cleaning on 50x50nm^2 area.

4.2. Annealing ambient

Bond energy is most often determined by two methods, the interface energy determination by measuring the crack length induced by inserting a blade between bonded surfaces as introduced by Maszara /22/ and by pull test of bonded wafers as it was performed in our case, due to lack of characterization equipment to perform the first one. The problem is that one can not determine directly the bonding energy with pull test method as in case of Maszara test, because there is no direct connection to tensile bond strength.

The influence of bond strengthening temperature and ambient on final bond quality was investigated by performing pull tests on 10x10 mm^2 samples. Bond tensile strength dependency versus temperature is presented in Fig.11 for all three ambients. In the presented temperature range two distinct regions are indicative. A

threshold temperature separating two regions is between 120°C-150°C, confirming the model of Tong. Below this temperature there is a region where successful bonding is not viable or it is in the range of only few tenths of MPa. Above this transition temperature the tensile strength only slightly increases and it saturates at the value around 10MPa, when the temperature approaches 400°C.

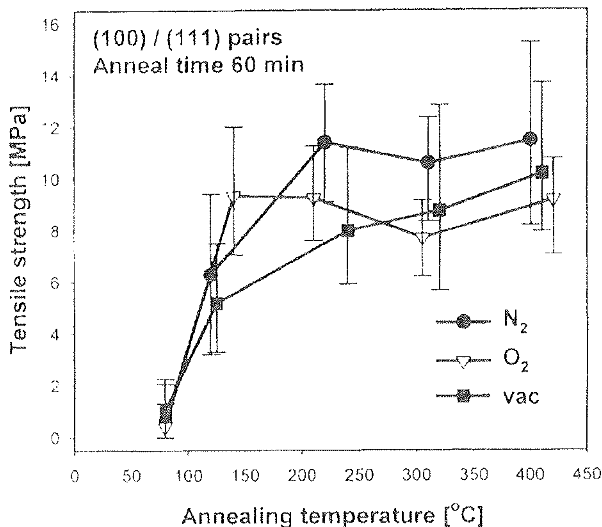

Fig.11: Bond tensile strength measurements as a result of increasing bonding temperature and three distinct bonding ambients. Native oxide on all surfaces is grown in HNO_3 at 110°C.

From Fig. 11 the difference between ambients utilized during bond annealing steps is evident. Inert nitrogen is showing the most encouraging results in our set of experiments. The reason for this is probably the fact that nitrogen as inert gas does not enter in any interface bonding reaction, therefore it neither supports nor inhibits the bonding mechanism itself once the pairs are mated.

Annealing in vacuum furnace in low vacuum range of 10Pa for 60 minutes did not strengthen the bond as it would be expected. These inferior results could be due to low vacuum range and low temperature, which possibly limit the mobility and outdiffusion of interface products. In contrast to the results of Tong, we did not observe the increased bonding strength due to the reduction of nitrogen at bonding interface in low vacuum ambient /14/. The possible disagreement could be as well due to annealing time difference, which could play a significant role in vacuum bonding conditions due to slow desorption of water from interface region.

In contrast to nitrogen, oxygen does enter the chemical reaction at the bonding interface as silicon oxidizing and binding species and can diffuse laterally through the interface, where it can also react with hydrogen to form additional water molecules. Oxygen plays a multiple role in bonding process as depicted in previous section. However, according to our results, shown in Fig.11, oxygen ambient does not participate to bond strengthening as an additional outer parameter, as was proposed by Lasky /1/, but on the contrary, suppresses the beneficial interface reactions for the chosen conditions. By cross-sectioning the bond interface, higher density of microvoids were found, thus correlating with poor tensile strength.

4.3. Crystal orientation

We focused more in detail into the fact that (100) and (111) oriented wafers have different surface termination, and thereby different number of available bonding sites according to steric hindrance /33/. (111) oriented silicon, with the most densely packed planes was expected to exhibit favorable bonding behavior with respect to (100) oriented wafers. However, for the purpose of wet micromachining, active wafer has to be (100) oriented. Some structures even require wet micromachining of support wafer and for this reason investigation on bonding of (100) to (100) oriented wafers was performed as well.

Following these ideas, several bonding experiments by pairing (100) and (111) surfaces, terminated with native chemical oxide and/or with thermal oxide as shown in Table 2 were performed. The results of bond quality of these experiments are shown in Fig. 12-14. Fig. 12 shows the case of bonding equal orientations. It was noticed that bonded (111)/(111) wafers exhibited higher tensile strengths at lower temperatures (150°C) and then decreased, reaching the values of bonded (100)/(100) wafer pairs. The stronger bonding ability around 150°C could be possibly attributed to higher density of bonding sites on adjacent surfaces due to the fact that native oxide is grown more rapidly and uniformly on (111) surfaces already at low temperature. Enhanced growth rate is probably supported by dissociation of interfacial water, diffusion through native oxide and further oxidation of the nonhomogeneously oxidized surface, making the initial chemical oxide structure laterally more homogeneous. A strong decrease of bond tensile strength was observed at around

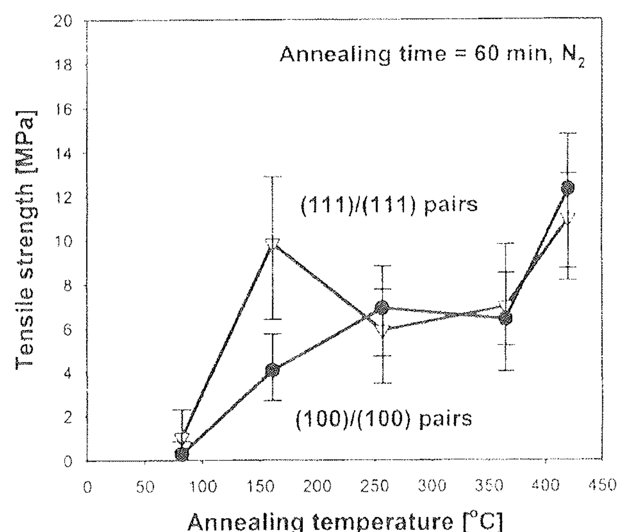

Fig.12: Bond tensile strength measurements versus increasing bonding temperature for (100)/(100) and (111)/(111) pairs. Native oxide was grown on all bonded surfaces in HNO_3 at 110°C.

250°C. Referring to Müller, the decrease is attributed to the void formation due to water release from the desorption and from the polymerization /6/. Subsequently, gradual increasing of bond tensile strength with temperature was noted for both pairs, reaching strength of 12MPa at 400°C. Saturation of bonding energy was not observed in this temperature range as was previously the case in bonding (111)/(100) pairs (Fig. 11).

Interesting results were obtained from the experiments where 253nm of thermal oxide grown on (100) wafer was bonded to (100) and (111) wafers with standard native oxide as described in Table 2. Results of temperature dependence of tensile bond strength are presented in Fig. 13. It is noteworthy that substantial gain in tensile strength of SiO_2/(111) over SiO_2/(100) bonding pairs was achieved at low temperatures between 160°C-250°C. The peak value of 20MPa was reached at temperature 160°C. As in previous case with (111)/(111) pairs, a substantial drop was again observed in the region between 200°C-300°C for SiO_2/(111) pairs. With increased temperature strength levels off and reaches together with SiO_2/(100) an equilibrium value of 8-10 MPa at 400°C that is about 20% less than in the case of bonding only native oxides. The possible explanation is that interface reaction products such as water now diffuse exclusively through the native oxide network creating new bonding sites, while hydrogen is dissolved in thermal oxide and thus increasing the bonding energy. At temperatures around 250°C and higher interfacial water has limited diffusion due to thicker native oxide and possible voids are formed, followed by bond tensile strength drop.

Fig. 14 presents bond tensile strength results depending on two different treatments in HNO_3. Pairs have been treated for 15 min at 110°C and 70°C, respectively. There is evident difference between two HNO_3 temperature treatments and related grown native oxides bonding behavior. Thicker and probably more homogeneous oxide was formed during higher temperature treatment. Latter promotes bonding more efficiently (almost doubles the tensile strength) via homogeneous distribution of bonding sites.

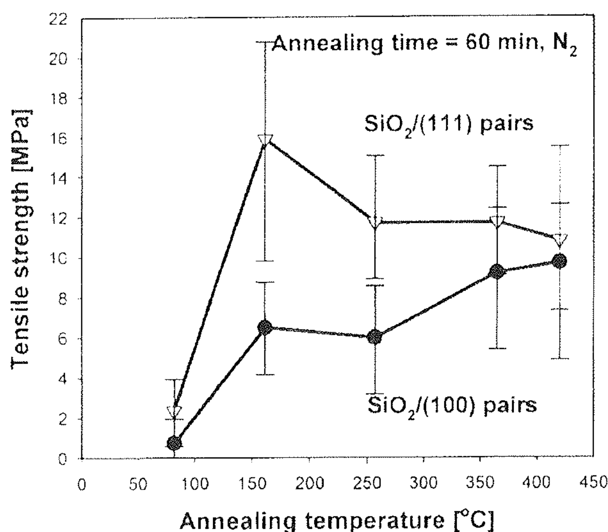

Fig.13: Bond tensile strength measurements versus increasing bonding temperature Bonding interface was native oxide on (100) / thermal SiO_2 and native oxide on (111) / thermal SiO_2.

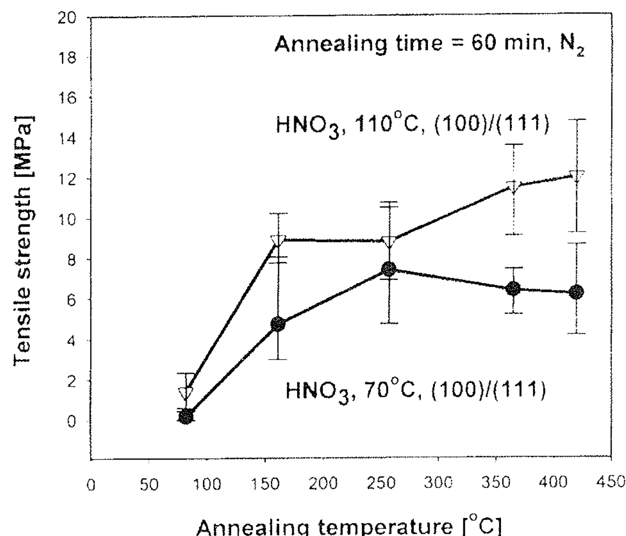

Fig. 14: Bond tensile strength measurements versus increasing bonding temperature for two different HNO_3 treatments. Thickness of grown native oxide was 0.8nm-1.2nm at 110°C and 0.5-0.6nm at 70°C.

4.5 Void inspection

In a temperature range of 200°C-700°C, voids are generated when hydrophilic surfaces are bonded /15,17/. At first it was proposed by some authors that bubbles are caused predominantly by water, which is a residue of physisorbed water after rearrangement at the interface and as the side product of condensation of OH groups when Si-O-Si bonds are formed /2,23,24/. It was also shown by the same authors that bubbles disappear or redissolve completely above 1000°C.

Methods that are commonly utilized to inspect this kind of macroscopic failures are as mentioned earlier, IR transmission imaging, x-ray diffraction topography, ultrasound microscopy and sometimes, beside the TEM investigation, the bond cross-section examination to obtain microscopic view. Infrared transmission imaging method is most often used to study the voids or imperfections at the bonding interface and was employed also in this study. Observations made during this investigation are in accordance with other authors, stating that origins of voids can be: i) particles left on the surface after cleaning that can be omitted by handling the wafers in cleanroom environment, ii) locally increased microroughness due to poor polishing or aggressive cleaning, or iii) trapped gases at the interface.

By destructive method of cross-sectioning of bonded samples additional information can be gained concerning the voids. Samples were diced and a short isotropic etching (3min) in mixture of HF-HNO_3-CH_3COOH (3:25:10) was performed to remove the damaged region, simultaneously enlarging and revealing individual voids at bonded interface. Fig.15 shows micrograph of a detail, revealing typical voids about 3-15μm in length, that were presented in samples annealed at 300°C in oxygen. Fig. 16 shows elliptic microvoid about 1μm long, that appeared in nitrogen annealed samples of

SiO_2/111 pairs at 400°C. Method itself is useful only for qualitative evaluation because only single line of cross section is examined, not the whole bonded area. No exact correlation could be found with tensile strength values, except for the case of oxygen annealing.

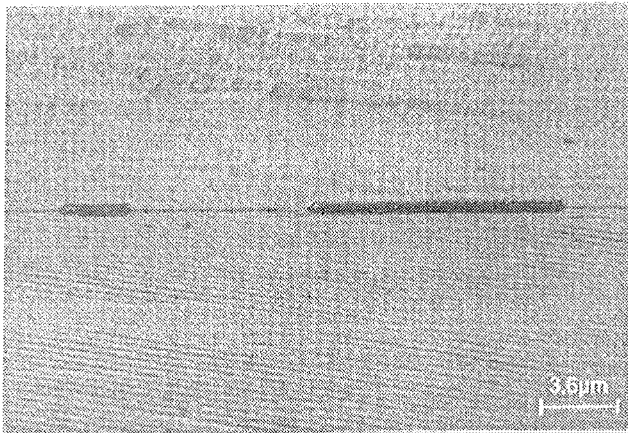

Fig.15: Cross-section of bonded sample in oxygen, revealing high density of voids that are presented at interface thus reducing the bond strength.

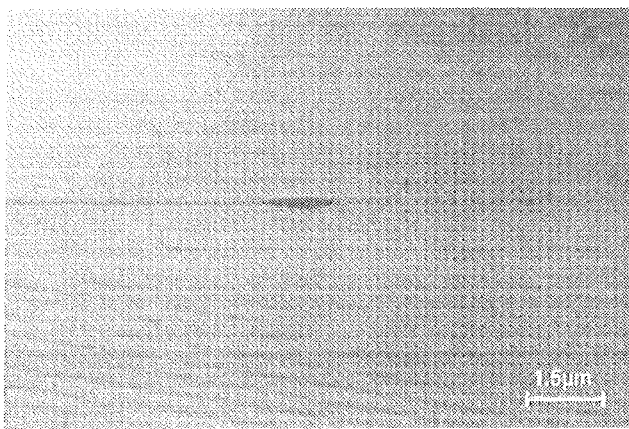

Fig.16: Cross-section of bonded sample in nitrogen, revealing low density of smaller voids that are presented at interface. Voids are actually smaller, enlargement follows from short isotropic etching.

Origins for bubble formation by Mitani could also be CH_x adsorbed groups that are adsorbed during handling and prolonged storage in plastic boxes /17/. This can be avoided by surface cleaning methods in plasma and to some extent in hot HNO_3. Avoiding any prolonged storage in plastic boxes or performing cleaning and bonding under high vacuum conditions is another solution. Hydrogen originating from dissociation process of interfacial water is also among possible origins, as it was confirmed by the experiment with liquid nitrogen by Tong /5/ and by Bengtsson /13/. It was shown that heating samples up to 600°C desorps hydrogen effectively.

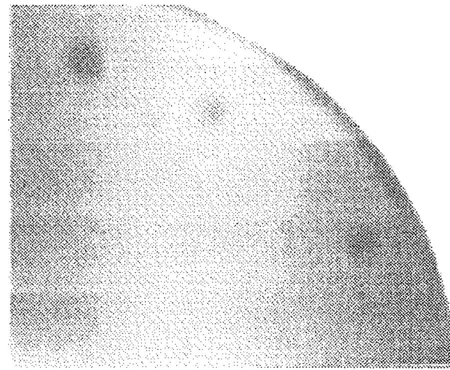

Fig.17: Infrared transmission image of bonding interface, treated at 400° in oxygen. Bubbles seen as dark spots were normally observed at the edge. Quarter of 3" wafer is presented.

By IR method also Newton fringes can be observed where particles are located. In our case none were observed confirming that cleaning and handling were appropriate. Attention was paid to the appearance of bubbles in samples bonded in different ambients to find a possible correlation to tensile strength results. Samples bonded at 400°C were investigated and only in case of bonded samples in oxygen ambient bubbles were observed as shown in Fig.17. Dark spots indicate change in absorption, i.e. trapped gases or imperfections in bonding interface. No bubbles were found in other samples bonded in vacuum and nitrogen, respectively. A drawback of this method, however is low spatial resolution meaning that microvoids can not be detected.

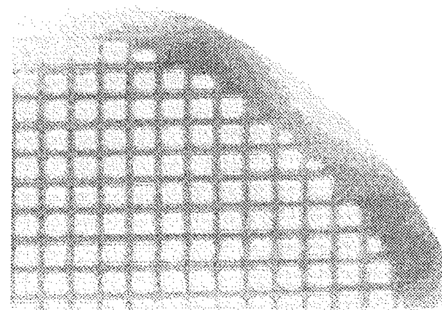

Fig.18: Infrared transmission images of bonded structure sample where micromachined pressure sensor was bonded to the support (111) oriented wafer.

Bonding of finalized pressure sensors at the waferscale was performed to apply the results of our investigation. Bonding was performed in low vacuum range. Micromachined cavities act as huge voids and the overall bonded area is small compared to the size of entire wafer. In case of low-pressure sensors, bonding of sensor rim is mandatory due to large size and fragile nature of thin diaphragm. Effective bond with the support wafer is represented only by small rim area and thereby has to assure strong enough and stable bond

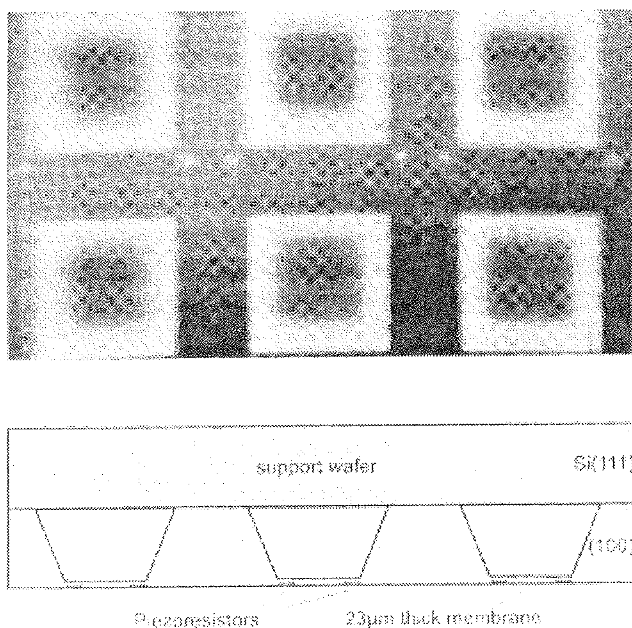

Fig.19: Infrared transmission images of bonded interface showing a detail from Fig. 18. with cross-section of whole microstructure. No microvoids could be detected with this method. Size of the membrane is 700x700µm^2. Ge lens with f=100mm was used for this case.

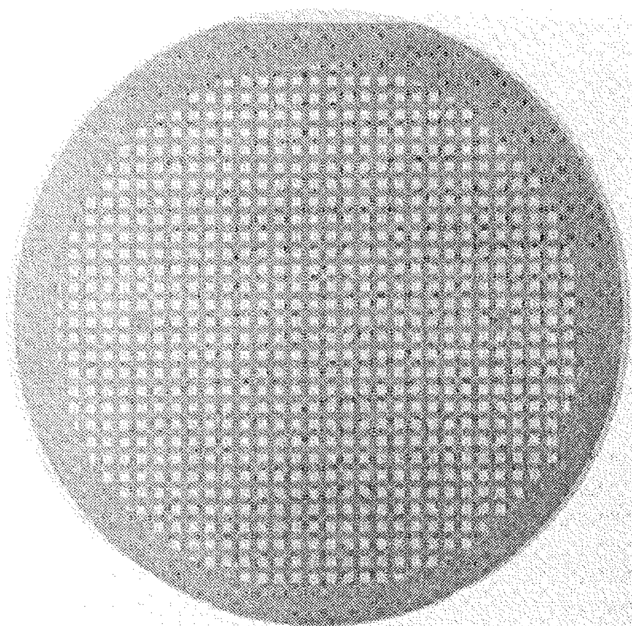

Fig. 20: X-ray image of bonded 3" wafer of completed pressure sensor to support (111) wafer in low vacuum (10Pa). Image exposure time was 3min and tube acceleration voltage was 90KV.

for the sensor in specific application. IR characterization of bond quality can also be used as nondestructive in-situ method in production and is therefore very promising. IR transmission image where active wafer with pressure sensors was bonded to (111) substrate wafer in a size of a quarter of 3" wafer is shown in Fig.18 and a detail of transmission image is presented in Fig.19 with adequate cross-section of the microstructure. Full size wafer to wafer bonding was additionally characterized by x-ray topography method and a photograph is shown in Fig. 20. No voids were detected by the setup adopted and as such revealed only huge cavities beneath the membrane, although the IR method did reveal minor nonhomogeneities.

4. Conclusions

Investigation of low temperature silicon-to-silicon waferscale direct bonding and potential role of (100) and (111) orientation in this process was performed in temperature range from 80°C to 400°C. Bonding energy was found to be rather poor below 120°C but it increases sharply above this temperature and saturates by approaching bond annealing temperature of 400°C. The influence of different bonding ambients such as oxygen, nitrogen or vacuum was investigated in the above temperature range. From experimental work it was determined that bond strengthening in nitrogen ambient exhibited about 25% higher tensile strength compared to bonding performed in vacuum or oxygen, which was in the range of 8-10 MPa.

(111)/(111) pairs terminated with native oxides showed higher bonding abilities compared to (100)/(100) pairs only at low temperatures indicating that additional bonding sites are created on (111) oriented surfaces, possibly due to additional oxidation of interface due to dissociated water resulting from interfacial reactions. Another contribution could be more hydrophilic nature of bonding surface due to higher positive charge in oxides grown on (111) surface compared to (100) surface.

It was found that the thickness of hydrous oxide grown in nitric acid at 110°C is sufficient to render a homogeneous and strong bond, while at lower temperatures of HNO_3 the grown oxide does not exhibit sufficient number of bonding sites and bonding energy is reduced.

Interesting results were obtained by pairing wafers with native oxide grown on different orientations to the wafers terminated with thermal SiO_2. Pairs SiO_2/(111) reached bond tensile strength value as high as 20MPa at 150°C and later dropped to a value comparable to SiO_2/(100) pairs which was around 10 MPa. Possible reduction of voids is due to enhanced diffusion of hydrogen into thermal oxide.

Roughness merely plays a role in bonding process if held within the limits of commercially available wafers. Increased microroughness caused by presented cleaning agents does not affect bonding at all. In most cases no voids were detected due to particles while hidrophilicity was sufficient. Cross-sectioning revealed microvoids, but no obvious correlation to tensile strength values were determined.

Acknowledgements

We are indebted to Dr. P. Panjan and Mr. J. Fric from the Josef Stefan Institute for performing surface profile measurements with surface profiler and AFM, respectively and to Mr. J. Hozjan from Fotona company for infrared transmission images. We owe our thanks also to Mr. K. Požun and Mr. A. Pregelj from IEVT for giving at our disposal vacuum furnace and to Dr. M. Klanjšek-Gunde from National Institute of Chemistry for valuable discussions. X-ray image was obtained with courtesy of Mr. N. Samsa from Institut za varilstvo, Ljubljana.

5. References

/1/ J. Lasky, Wafer bonding for silicon-on-insulator technologies, Appl. Phys. Lett. 48 (1), 6 January 1986, 78-80

/2/ M. Shimbo, K. Furukawa, K. Fukuda, K. Tanzawa, Silicon-to-silicon direct bonding method, J. Appl. Phys. 60 (8), 15 October 1986, 2987-2989

/3/ L. Ristic, editor, Sensor technology and devices, Artech House, Boston, 1994.

/4/ S.M. Sze,editor, Semiconductor sensors, John Wiley & sons, Inc., New York, 1994.

/5/ Q.-Y. Tong, G. Cha, R. Gafiteanu, U. Gösele, Low temperature wafer direct bonding, J. of Microelectromech. Systems, Vol. 3, No. 1, March 1994, 29-35

/6/ B. Müller and A. Stoffel, Tensile strength characterization of low-temperature fusion- bonded wafers, J. Micromechanical Microengineering, 1, 1991,161-166

/7/ A. Berthold, M.J.Vellekop, IC compatible silicon wafer to wafer bonding, Sensors and Actuators, A60, 1997, 208-211

/8/ J. Jiao, D. Lu, B. Xiong, W. Wang, Low temperature silicon direct bonding and interface behaviors, Sensors and Actuators, A50, 1995, 117-120

/9/ G. Krauter, A. Schumacher, U. Gösele, Low temperature silicon direct bonding for application in micromechanics: bonding energies for different combinations of oxides, Sensors and Actuators, A 70, (1998), 271-275

/10/ H. Takagi, R. Maeda, T.R. Chung, T. Suga, Low temperature direct bonding of silicon dioxide by the surface activation method, Sensors and Actuators A70, (1998), 164-170

/11/ S.N. Farrens, J.R. Dekker, J.K. Smith, B.E. Roberds, Chemical free room temperature wafer to wafer bonding, J.Electrochem. Soc., Vol 142, No. 11, November 1995, 3949-3955

/12/ U. Gösele, H.Stenzel, T. Martini, J.Steinkirchner, D. Conrad, K. Scheerschmidt, Self-propagating room-temperature silicon wafer bonding in ultrahigh vacuum, Appl. Phys. Lett. 67 (24), 11 December 1995, 3614-3616

/13/ S.Bengtsson, O. Engstrom, Low-temperature preparation of silicon/silicon interfaces by the silicon-to-silicon direct bonding method, J.Electrochem. Soc., Vol 137, No. 7, July 1990, 2297-2303

/14/ Q.-Y. Tong, W.J. Kim, T.-H. Lee, and U. Gösele, Low Vacuum Wafer Bonding, Electrochemical and Solid State Letters, Vol.1 (1998), 52-53

/15/ G. Kissinger and W. Kissinger, Void free silicon wafer bond strengthening in the 200-400°C range, Sensors and Actuators, A36, 1993, 149-156

/16/ K. Hermansson, F. Grey, S. Bengtsson, U. Sodervall, Ultraclean Si/Si interface formation by surface preparation and direct bonding in ultrahigh vacuum, J.Electrochem. Soc., Vol 145, No. 5, May 1998, 1645-1649

/17/ K. Mitani, V. Lehmann, R. Stengl, D. Feijoo, U.M. Gösele, H.Z. Massoud, Causes and prevention of temperature-dependent bubbles in silicon wafer bonding, Jap. Journal of Appl. Phys., Vol. 30, No 4, April, 1991, 615-622

/18/ M. Miyashita, T. Tusga, K. Makihara, T. Ohmi, Dependence of surface Microroughness of CZ, FZ, and EPI wafers on wet chemical processing, J.Electrochem. Soc., Vol 139, No. 8, August 1992, 2133-2142

/19/ T. Hattori, K. Takase, H. Yamagishi, R. Sugino, Y. Nara, T. Ito, Chemical structures of native oxides formed during wet chemical treatments, Jap. Journal of Appl. Phys., Vol. 28, No. 2, February 1989, L296-L298

/20/ C. Harendt, B. Hofflinger, H.-G. Graf, E. Penteker, Silicon direct bonding for sensor application: Characterization of bond quality, Sensors and Actuators A, 25-27, (1991), 87-92

/21/ C. Harendt, H.-G. Graf, E. Penteker, B. Hofflinger, Wafer bonding: Investigation and in situ observation of the bond process, Sensors and Actuators A, 21-23, (1990), 927-930

/22/ W.P Maszara, G. Goetz, A. Caviglia, J.B. Mc Kitterick, Bonding of silicon wafers for silicon-on-insulator, J.Appl.Phys. 64 (10), 15 November 1989, 4943-4950

/23/ R. Stengl, T Tan, U. Gösele, A model for the silicon wafer bonding process, Jap. Journal of Appl. Phys., Vol. 28, No. 10, October 1989, 1735-1741

/24/ T. Abe, T. Takei, A. Uchiyama, K. Yoshizawa, Y. Nakazato, Silicon wafer bonding mechanism for silicon-on -insulator structures, Jap. Journal of Appl. Phys., Vol. 29, No 12, December, 1990, pp. L2311-L2314

/25/ Q.-Tong and U. Gösele, A Model of Low Temperature Wafer Bonding and Its Applications, Journal of Electrochemical Society, Vol. 143, No.5, May 1996, 1773-1779

/26/ G. Kissinger and W. Kissinger, Hydrophylicity of Silicon Wafers for Direct Bonding, Phys. Stat. Sol. (a) 123, 1991, 185-192

/27/ T. Aoyama, T. Yamazaki, T. Ito, Nonuniformities of native oxides on Si(001) surfaces formed during wet chemical cleaning, Appl. Phys. Lett. 61 (1), 6 July 1992, 102-104

/28/ Y. Bäcklund, K. Hermansson, L. Smith, Bond-Strength measurements related to silicon surface hydrophilicity, J.Electrochem. Soc., Vol 139, No. 8, August 1992, 2299-2301

/29/ M.K. Weldon, W.E. Marsico, Y.J. Chabal, D.R. Hamann, S.B. Christman, E.E. Chaban, Infrared spectroscopy as a probe of fundamental processes in microelectronics: silicon wafer cleaning and bonding, Surface Science 368, (1996), 163-178

/30/ W.P Maszara, B.-L. Jiang, A. Yamada, G.A Rozgony, H. Baumgart, A.J.R. de Kock, Role of surface morphology in wafer bonding, J.Appl. Phys. 69 (1), 1, January 1991, 257-260

/31/ T.A. Michalske, B.C. Bunker, Slow fracture model based on strained silicate structures, J. Appl. Phys. 56 (10), 15 November 1984, 2686-2693

/32/ K. Mitani and U.M. Gösele, Wafer Bonding Technology for Silicon-on-Insulator Applications: A Review, Journal of Electronic Materials, Vol. 21, No. 7, 1992, 669-676

/33/ F. Shimura, Semiconductor silicon crystal technology, Academic press, Inc., San Diego, 1989

/34/ A. Satoh, Water glass bonding, Sensors and Actuators A72, (1999), 160-168

/35/ A. Plössl, G. Krauter, Wafer direct bonding: tailoring adhesion between brittle materials, Mat. Sci. Engineering, R25, No. 1-2, March 1999, 1-88

mag. Drago Resnik, dipl.ing.,
mag. Danilo Vrtačnik, dipl. ing.,
mag. Uroš Aljančič, dipl.ing. and dr. Slavko Amon
Laboratorij za Mikrosenzorske strukture,
Fakulteta za Elektrotehniko, Ljubljana, Slovenia
Laboratory of Microsensor Structures,
Faculty of Electrical Engineering,
Tržaška 25, Ljubljana 1000, SLOVENIA
Tel. +386 61 1768 303,
Fax. +386 61 1264 630,
E-mail: Drago.Resnik@fe.uni-lj.si

Prispelo (Arrived): 9.2.00 *Sprejeto (Accepted): 29.2.00*